To appear in *European Journal of Environmental and Civil Engineering*
Vol. 00, No. 00, Month 20XX, 1–25

A simplified model for railway catenary-wire dynamics

Antonio Cazzani[a]*, Marco Cattani[b], Raffaele Mauro[c] and Flavio Stochino[a,d]

[a]*Department of Civil and Environmental Engineering and Architecture, University of Cagliari, Cagliari, Italy*
[b]*Trentino Mobilità S.p.A., Trento, Italy*
[c]*Department of Civil, Environmental and Mechanical Engineering, University of Trento, Trento, Italy*
[d]*Department of Architecture Design and Urban Planning, University of Sassari, Alghero, Italy*

(*December 23, 2015*)

In this paper a simplified analytic model for the dynamic behavior of railway catenary wire is presented. The model is discussed and validated with the help of numerical results obtained by a finite element code, for the case of a typical Italian railway installation.

The simplified model is convenient from the computational point of view and is useful for sensitivity analysis. Some parametric studies have been developed by considering as free parameters the velocity and the distance of the train pantographs and looking at their effect on catenary dynamics.

Keywords: wire dynamics, catenary-pantograph interaction, dynamics of taut cables, railway installation optimization, modal analysis, analytic model, continuous elastic support.

1. Introduction

Critical infrastructures like railways, bridges and strategic buildings are required to be extremely reliable to avoid the high social costs of their failure: for this reason a thorough design of each part and of their combined working conditions is required. This process can be applied at each stage of the design procedure, considering all the possible risks and the corresponding reduction strategies, see for instance Hamzaoui et al. (2015).

In the case of high speed railways, the power supply wire system is of paramount relevance: the required high performance level is strongly influenced by its electro-mechanical system. In most cases it is realized by means of pantograph, mounted on the roof of the train, which runs in contact with an overhead wire that is linked to the catenary rope by means of vertical droppers. The catenary is supported by piles fixed in the ground. In this way the electrical power flows from the wire to the train engine in a circuit which is closed by the tracks. The technical development of pantograph and its interaction with the catenary is a current research issue in railway engineering with an increasing importance due to the development of high speed infrastructures.

*Corresponding author. Email: antonio.cazzani@unica.it

Please cite this document as: A. Cazzani, M. Cattani, R. Mauro, F. Stochino "A simplified model for railway catenary-wire dynamics " *European Journal of Environmental and Civil Engineering* , 2017, 21(7–8): 936–959
DOI:10.1080/19648189.2016.1245631

The pantograph applies an upward force to the contact wire that is consequently moved upwards. This displacement is not constant along the wire, which presents a variable stiffness because the zone near the supports are stiffer than the others. Thus the pantograph must move up and down following the wire and these movements are reduced by its translational inertia which becomes bigger as velocity increases. In this way the interaction force applied to the wire is not constant too and, in some cases, it becomes negligible, resulting in the detachment of the pantograph. This situation is extremely dangerous not only because of localized wear in the cables and in the pantograph due to electric arc phenomena but also because of voltage spikes in the electric engine.

The scientific literature concerning pantograph-catenary system interaction is wide and an increasing number of papers have been published in the recent past, as the importance of high speed trains has grown. An interesting review paper by Poetsch et al. (1997) critically presents an effective analysis of the dynamics of this mechanical system and looks at the models proposed in the literature outlining their advantages and disadvantages.

In the published contributions it is possible to distinguish between analytical and numerical approaches. Several former papers were devoted to string models, Andrews (1964), Gilbert and Davies (1966), Hobbs, Illingworth, and Peters (1977), Manabe and Fujii (1990), Renger (1990), Resch (1991), Bianchi and Tacci (1991), Brodkorb and Semrau (1993), Greco, Impollonia, and Cuomo (2014). Other authors have instead modeled the catenary as a beam, considering also its bending stiffness, *e.g.* Levy, Bain, and Leclerc (1968), Becker et al. (1995) and, more recently, Seo et al. (2006). The differences between these two approaches have been analyzed in the aforementioned review by Poetsch et al. (1997). There, the authors state that the effect of bending stiffness is important especially in the case of high-frequency contact processes (wrinkling, contact breaks). In fact, neglecting bending stiffness, will hardly influence simulation results with respect to the low-frequency behavior.

In the group of analytic solutions, a special mention can be devoted to the single degree-of-freedom (SDOF) models proposed by Wu and Brennan (1998) and Wu and Brennan (1999). In these papers a dynamic stability analysis is developed considering also the dynamic stiffness of the catenary and its influence on the overall behavior of the mechanical system. The dynamic stiffness of the catenary constituting the overhead wire system has often been represented by an infinite, periodically spring-supported, string. Another analytic simplified model characterized by lumped mass is presented in an early work by Nibler (1950). More recently, the steady state vibration of a periodically supported structure is developed by Metrikine, Wolfert, and Vrouwenvelder (1999) with a particular attention to the effects of load velocity on the dynamic response.

Other cable vibration problems, including the effects of wind-induced excitations, galloping and aeroelastic instability have been addressed, among others, by Zulli and Luongo (2012), Piccardo, Pagnini, and Tubino (2015), Piccardo, Tubino, and Luongo (2016). On the other hand, the more general effects of traveling masses — and not only of traveling forces, which is the case of this paper and of a preliminary version of it, see Cattani, Cazzani, and Mauro (2000), which appeared (in Italian only) some years ago — have been considered in Ferretti and Piccardo (2013) for the case of taut strings and in Cazzani et al. (2016b) for the case of plane-curved beams.

Unfortunately, an analytical solution of the catenary problem, cannot be found for each case and for each geometry; indeed, if the transient solution is sought, numerical methods become of paramount relevance. In the past several researchers have found numerical solutions to these problems by means of the finite difference approach: among them Andrews (1964), Scott and Rothman (1974), Oda, Morikawa, and Kusumi (1986). In particular in Arnold and Simeon (2000), the non-linear interaction between the catenary system and the pantograph is analyzed by means of a simplified model where the

Please cite this document as: A. Cazzani, M. Cattani, R. Mauro, F. Stochino "A simplified model for railway catenary-wire dynamics " *European Journal of Environmental and Civil Engineering* , 2017, 21(7–8): 936–959
DOI:10.1080/19648189.2016.1245631

equations of motion are discretized in the space via finite differences while time discretization is obtained with Differential Algebraic Techniques (DAE).

Currently, the largest number of papers concerning railway catenary behavior exploits the Finite Element Method (FEM): see, for instance, Bianchi and Tacci (1991), Reinbold and Deckart (1996) and, more recently, Andreu, Gil, and Roca (2006) where the formulation of a deformable catenary element is presented, or Park, Han, and Jang (2003) where a thorough sensitivity analysis of the problem parameters is developed in order to maximize pantograph performance. In Veylon and Gual (2003) an interesting comparison between the FEM model and the corresponding analytical one is presented for the case of a vibrating string.

Another approach consists of representing the catenary vibration as the superposition of a finite number of exact or estimated eigenfunctions which are continuous in space. This approach was widely adopted in the past, see for example: Levy, Bain, and Leclerc (1968), Hobbs, Illingworth, and Peters (1977), Renger (1990), Brodkorb and Semrau (1993).

It is conceivable that damping for this considered type of structures could be achieved by adopting smart and/or micro-structured materials; for the former group the problems of vibration control and wave propagation have been studied, for instance by Rosi, Pouget, and dell'Isola (2010) and dell'Isola, Madeo, and Placidi (2012) in the case of solids, and by dell'Isola, Giorgio, and Andreaus (2015), dell'Isola et al. (2016a), Madeo et al. (2015) for lattice-beam structures (see for more details about the features of these lattice systems, dell'Isola et al. (2016b), Scerrato et al. (2016)); for the latter group, similar researches have been carried out by Eremeyev et al. (2007), Rosi, Giorgio, and Eremeyev (2013), Berezovski, Giorgio, and Della Corte (2016).

In a static framework Lopez-Garcia, Carnicero, and Torres (2006) and Such et al. (2009) presented a non-linear analysis for 3-D catenaries taking into account cable elasticity and obtaining a high numerical efficiency. An interesting optimization technique was recently applied to similar problems by Wang and Qin (2016). In this case, the best shape of cables distribution in a suspension bridge is assessed in a non-linear framework using the interacting matrix theory. Of course, very interesting technological applications might include either contact problems or the analysis of vibrations induced by impact or impulsive loads: some meaningful contributions in this field are due to Acito, Stochino, and Tattoni (2011), Andreaus, Chiaia, and Placidi (2013), Stochino (2016), Andreaus, Baragatti, and Placidi (2016).

In this paper a simplified catenary model is presented, which is based on a multi-span string on a continuous Winkler-type elastic support. The equation of motion is solved by separation of variables, so that a closed-form solution of the catenary dynamic problem expressed by means of a finite number of vibration modes is obtained. In particular, the case of a constant force, traveling at a constant speed along the string is considered, which corresponds to the ideal case of a mass-less pantograph. The other hypotheses of this simplified model, which is presented in detail is Section 2, are: (*i*) a linearization of the taut string model; (*ii*) a simplification to a single, elastically supported, wire of the real catenary, which includes contact wire, droppers and catenary rope.

Then, in Section 3, the analytical solution of the problem is obtained while in Section 4 the calibration of the simplified model stiffness coefficients, and equivalent mass is developed, by referring to a FE model. Simplified model validation is assessed in Section 5 by means of a direct comparison with a FE numerical model. Finally, in Section 6 a parametric analysis of the pantograph-catenary dynamics is developed in order to propose a design procedure for new railways. Some concluding remarks and prospective analysis are stated in Section 7.

Please cite this document as: A. Cazzani, M. Cattani, R. Mauro, F. Stochino "A simplified model for railway catenary-wire dynamics " *European Journal of Environmental and Civil Engineering* , 2017, 21(7–8): 936–959
DOI:10.1080/19648189.2016.1245631

2. Model description

In the simplified model the system composed of the catenary rope connected to the contact wire by the droppers is represented by a single straight wire with uniform mass and tension. Appropriate boundary conditions (BCs) are applied to the wire in order to take into account the effects of droppers. The vibration of a taut string is expressed by the following hyperbolic partial differential equation (PDE), see Bishop and Johnson (1960) or Wang and Wang (2013):

$$m\frac{\partial^2 y\left(x,t\right)}{\partial t^2} = T\frac{\partial^2 y\left(x,t\right)}{\partial x^2} + p\left(x,t\right), \tag{1}$$

where y represents the vertical displacement, m the mass per unit length, T the traction force and p the vertical load per unit length applied to the wire. Eq. (1) is a balance equation of forces which are applied to the originally horizontal wire and acting along the transversal (*i.e.* vertical) direction: the inertia term is recognized in the l.h.s., while on the r.h.s. there appear the vertical component of the tensile force, which is computed according to a linearized expression for the angle formed by the local tangent direction of the string and the horizontal (longitudinal) direction, and the applied external load, which is assumed to be positive if directed upwards. The effect of droppers which connect the catenary rope to the contact wire is represented, see Figure 1, by a continuous elastic support, whose distributed stiffness is denoted by k. For this reason it is necessary to introduce in Eq. (1) this contribution:

$$m\frac{\partial^2 y\left(x,t\right)}{\partial t^2} + ky\left(x,t\right) = T\frac{\partial^2 y\left(x,t\right)}{\partial x^2} + p\left(x,t\right). \tag{2}$$

This governing equation is the counterpart of that ruling the behavior of a beam on elastic support following Winkler's model, see for instance Ding (1993) (for the case of a complete elastic support) or Cazzani (2013) (for the case of a partial one).

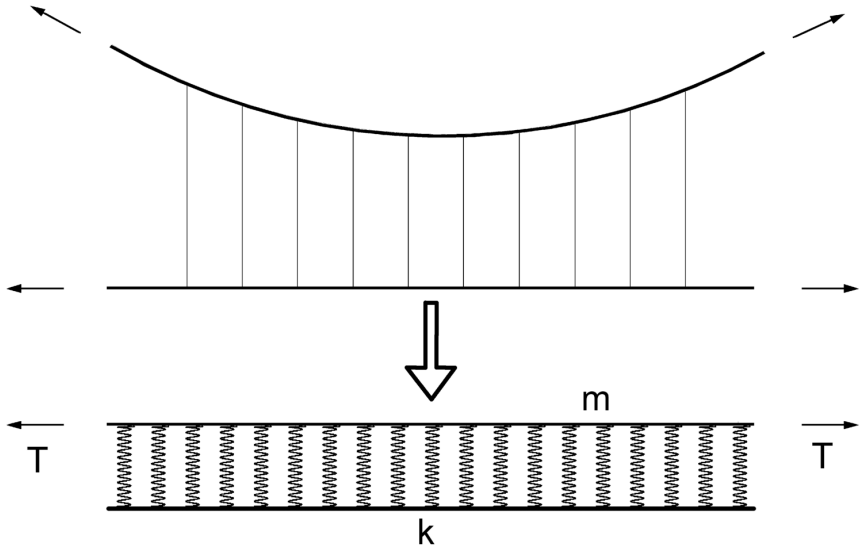

Figure 1. Model of a taut string on a continuous elastic support (k is the distributed stiffness coefficient).

The presence of the term $ky\left(x,t\right)$ doesn't prevent obtaining a closed-form solution to Eq. (2). Indeed it is represented, as in the case of Eq. (1), by a sum of eigenfunctions. The

Please cite this document as: A. Cazzani, M. Cattani, R. Mauro, F. Stochino "A simplified model for railway catenary-wire dynamics " *European Journal of Environmental and Civil Engineering* , 2017, 21(7–8): 936–959
DOI:10.1080/19648189.2016.1245631

influence on the stiffness of the supporting piles is expressed on the model by a pair of localized (*i.e.* concentrated) elastic supports (see Figure 2) characterized by a stiffness coefficient K and located in correspondence to the nearest droppers. Indeed in these points the highest value of the catenary stiffness is detected. It has to be noticed that as many concentrated elastic supports as the number of droppers should be introduced, in principle, but the effect of those far from the piles is neglected consistently with the degree of approximation of the simplified model.

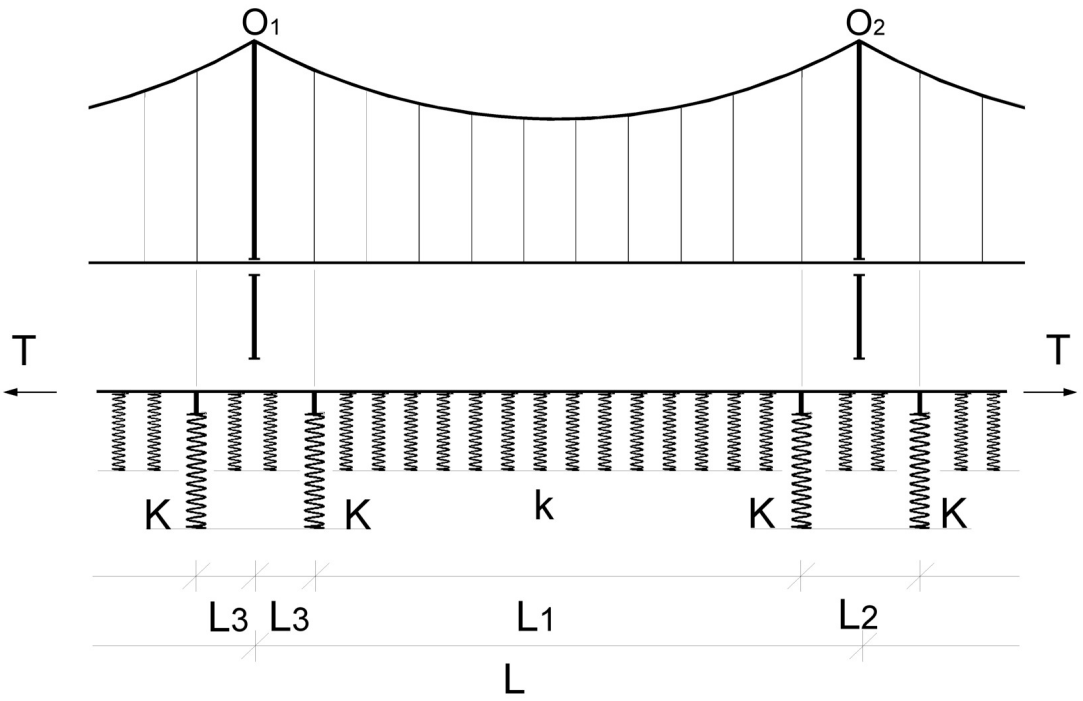

Figure 2. Model of a taut string on a continuous elastic support (whose stiffness is k) representing the real catenary system shown above. Springs with stiffness K represent the localized elastic support provided by the first and the last droppers, close to the suspension points (O_1, O_2) of the catenary wire. L_3 denotes the distance from the suspension point O_1 (or O_2) to the first/last dropper; $L_2 = 2L_3$ is the distance between the last dropper of one span and the first dropper of the next one.

The presence of these supports doesn't modify the problem equation which is still represented by Eq. (2): indeed the effect of such localized elastic support can be expressed by appropriate boundary conditions.

3. Solution of the governing PDE

The solution to Eq. (2) can be labeled as $y(x,t)$. It represents the time-history of the vertical displacements of the catenary-wire as a function of the longitudinal abscissa x. This function can be determined by the method of separation of variables, which yields:

$$y(x,t) = \Psi(x)g(t). \tag{3}$$

In this way, the solution is composed of a function $\Psi(x)$ (*eigenfunction*) that depends on the position and describes the vibration modes (*eigenmodes*) of the taut string, and by a function $g(t)$, which depends on the time t. The latter takes into account how the combination of eigenmodes changes during the oscillation process. The eigenmodes

Please cite this document as: A. Cazzani, M. Cattani, R. Mauro, F. Stochino "A simplified model for railway catenary-wire dynamics " *European Journal of Environmental and Civil Engineering* , 2017, 21(7–8): 936–959
DOI:10.1080/19648189.2016.1245631

are characteristics of the structure (the taut string considered with its boundaries) and depend on the mass density m, traction T, length L and stiffness coefficients, k and K.

An eigenfrequency is associated to each eigenmode and represents the frequency of that particular vibration mode. In order to determine eigenfrequencies and eigenmodes the homogeneous equation associated to Eq. (2) with the appropriate boundary conditions is considered. Introducing Eq. (3) into Eq. (2) and disregarding external loads, *i.e.* assuming $p\,(x,t) = 0$ gives:

$$m\,\Psi(x)\frac{d^2g(t)}{dt^2} + k\,\Psi(x)g(t) = T\,\frac{d^2\Psi(x)}{dx^2}g(t). \tag{4}$$

From now on, a short-hand notation is adopted, such that time derivatives will be denoted by a superposed dot on the relevant function, *e.g.* :

$$\dot{g}(t) = \frac{dg(t)}{dt}, \qquad \ddot{g}(t) = \frac{d^2g(t)}{dt^2},$$

and similarly derivatives with reference to the space variable x will be distinguished by primes, for instance:

$$\Psi'(x) = \frac{d\Psi(x)}{dx}, \qquad \Psi''(x) = \frac{d^2\Psi(x)}{dx^2}.$$

The traditional, extended notation will be still used only in those case where ambiguity might arise. Thus Eq. (4) is written equivalently as:

$$m\Psi(x)\ddot{g}(t) + k\Psi(x)g(t) = Tg(t)\Psi''(x). \tag{5}$$

It can be proved (see Appendix A) that Eq. (5) is equivalent to a set of two ordinary differential equations (ODEs):

$$\begin{cases} \ddot{g}(t) + \omega^2 g(t) = 0, \\ \Psi''(x) + \dfrac{m\omega^2 - k}{T}\Psi(x) = 0. \end{cases} \tag{6}$$

These Eqs. (6) can be solved separately; the former solution $g(t)$ expresses the time-history of the coefficients $g_n(t)$ corresponding to the eigenfunctions $\Psi_n(x)$, see Eq. (3) which, for each natural vibration mode n, *i.e.* for any eigenfrequency ω_n, can be obtained from the solution of the latter equation. To this purpose, the solution can be expressed by assuming

$$\alpha_n^2 = \frac{m\omega_n^2 - k}{T}. \tag{7}$$

Then for the case of a single span string it follows the ODE:

$$\Psi_n''(x) + \alpha_n^2\Psi_n(x) = 0, \tag{8}$$

whose solution can be shown to be:

$$\Psi_n(x_i) = A_n\cos\alpha_n x + B_n\sin\alpha_n x. \tag{9}$$

Please cite this document as: A. Cazzani, M. Cattani, R. Mauro, F. Stochino "A simplified model for railway catenary-wire dynamics " *European Journal of Environmental and Civil Engineering* , 2017, 21(7–8): 936–959
DOI:10.1080/19648189.2016.1245631

Constants A_n, B_n can be evaluated enforcing boundary conditions and solving the corresponding homogenous system of linear algebraic equations which provide non-trivial solutions only for particular values of α_n. In the case of multiple spans, the need of enforcing boundary conditions at the end of each span yields to the definition of the eigenmode by means of local coordinates on each single span. Eq. (9) is then constructed by joining separate functions $\Psi_{n,i}(x_i)$, each of them being defined on a separate, independent domain $0 \leq x_i \leq l_i$, so that $\Psi_{n,i}(x_i)$ is the restriction of $\Psi_n(x)$ when x lies within the i-th domain. Hence, it follows:

$$\Psi_{n,i}(x) = A_{n,i} \cos \alpha_n x_i + B_{n,i} \sin \alpha_n x_i. \tag{10}$$

The boundary conditions for the system depicted in Figure 2 require that displacement continuity and equilibrium in the vertical direction are fulfilled at the location of each elastic support; from the mathematical point of view these boundary conditions produce:

$$\Psi_{n,i}(0) = \Psi_{n,i-1}(l_i), \tag{11}$$

$$T \left. \frac{\Psi_{n,i}}{dx_i} \right|_0 - T \left. \frac{\Psi_{n,i-1}}{dx_{i-1}} \right|_{l_i} = K \Psi_{n,i}(0), \tag{12}$$

where index n denotes the n-th eigenfunction and i represents the catenary portion bounded by two consecutive elastic supports. Indeed the eigenfunction are expressed by joining different function defined on different domains and characterized by different values of constant $A_{n,i}$ and $B_{n,i}$.

For a catenary which extends over p *complete spans* (those delimited by suspension points O_1, O_2, etc.), each of them with an overall length L, see Figure 2, this approach requires considering $2p + 1$ sections (or *single spans*). Indeed, the concentrated elastic supports acting on the equivalent wire are not located at the ends of the complete span, but at a distance L_3 from both ends. Hence the string model is subdivided in a larger number of portions: their number amounts to $2p + 1$. In particular, looking at Figure 2, this comes out to be the typical sequence of single span lengths: $l_1 = L_3$, $l_2 = L_1$, $l_3 = L_2$, $l_4 = L_1$, $\ldots$, $l_{2p-1} = L_2$, $l_{2p} = L_1$; $l_{2p+1} = L_3$. As a consequence, the unknown constants ($A_{n,i}$ and $B_{n,i}$), which are two for each single span, turn out to be $4p + 2$. The corresponding $4p + 2$ equations can be obtained writing Eqs. (11) and (12) for each of the $2p$ internal supports (these provide $4p$ equations) and considering the outer boundary conditions for the whole catenary, which give two more equations. These outer boundary conditions express the requirement that the catenary is fixed at both ends, namely: $\Psi_{n,1}(x_1 = 0) = 0$, $\Psi_{n,2p+1}(L_3) = 0$.

Together these conditions yield a system of homogeneous linear algebraic equations which allows to evaluate the eigenfrequency and the corresponding vibration modes (eigenmodes):

$$\mathbf{D}(\alpha_n)\mathbf{X}_n = \mathbf{0}. \tag{13}$$

Indeed, Eq. (13) represents a typical eigenproblem: vector $\mathbf{X}$ (the eigenvector) collects componentwise the integration constants which are relevant to all single spans, namely:

$$\mathbf{X}_n = \left\{ A_{n,1} \;\; B_{n,1} \;\; \ldots \;\; A_{n,i} \;\; B_{n,i} \;\; \ldots \;\; A_{n,2p+1} \;\; B_{n,2p+1} \right\}^T, \tag{14}$$

The corresponding square system matrix $\mathbf{D}$, whose dimensions are $(4p + 2) \times (4p + 2)$,

Please cite this document as: A. Cazzani, M. Cattani, R. Mauro, F. Stochino "A simplified model for railway catenary-wire dynamics " *European Journal of Environmental and Civil Engineering* , 2017, 21(7–8): 936–959
DOI:10.1080/19648189.2016.1245631

depends on α; for those particular values $\alpha = \alpha_n$ (the eigenvalues) such that matrix $\mathbf{D}$ becomes singular, free vibrations can occur for the system. For the specific case when, as already mentioned, both outer boundaries are fixed, the expression of the system matrix is the following:

$$\mathbf{D} = \begin{bmatrix} 1 & 0 & 0 & 0 & 0 & 0 & 0 & 0 & \cdots & 0 \\ C_3 & S_3 & -1 & 0 & 0 & 0 & 0 & 0 & \cdots & 0 \\ \alpha T S_3 & -\alpha T C_3 & -K & \alpha T & 0 & 0 & 0 & 0 & \cdots & 0 \\ 0 & 0 & C_1 & S_1 & -1 & 0 & 0 & 0 & \cdots & 0 \\ 0 & 0 & \alpha T S_1 & -\alpha T C_1 & -K & \alpha T & 0 & 0 & \cdots & 0 \\ 0 & 0 & 0 & 0 & C_2 & S_2 & -1 & 0 & \cdots & 0 \\ 0 & 0 & 0 & 0 & \alpha T S_2 & -\alpha T C_2 & -K & \alpha T & \cdots & 0 \\ \cdots & \cdots & \cdots & \cdots & \cdots & \cdots & \cdots & \cdots & \cdots & \cdots \\ 0 & 0 & 0 & 0 & 0 & \cdots & C_1 & S_1 & -1 & 0 \\ 0 & 0 & 0 & 0 & 0 & \cdots & \alpha T S_1 & -\alpha T C_1 & -K & \alpha T \\ 0 & 0 & 0 & 0 & 0 & \cdots & 0 & 0 & C_3 & S_3 \end{bmatrix}, \tag{15}$$

where $S_j = \sin \alpha L_j$ and $C_j = \cos \alpha L_j$.

The first two columns refer to the coefficients corresponding to $A_{n,1}$ and $B_{n,1}$ associated with the first single span of the catenary, whose length is L_3, see Figure 2. In the same way, the following pairs of columns refer to span length respectively equal to L_1 and L_2; the last couple of columns is referred again to a span length equal to L_3 and corresponds to coefficients $A_{n,2p+1}$ and $B_{n,2p+1}$.

So, the eigenfrequencies are linked to those particular values $\alpha = \alpha_n$, which make matrix $\mathbf{D}$, appearing in Eq. (13), singular. An eigenmode is associated to each value α_n. In order to determine each eigenmode the corresponding value of α_n is enforced in Eq. (13) obtaining the corresponding vector $\mathbf{X}_n$, which is defined to within an arbitrary amplitude factor. Once $\mathbf{X}_n$ is known and has been properly normalized, the relevant vibration mode (eigenmode) can be constructed piece by piece in the following way:

$$\Psi_n(x) = \begin{cases} A_{n,1} \cos \alpha_n x_1 + B_{n,1} \sin \alpha_n x_1 & (0 \le x_1 \le l_1) \\ A_{n,2} \cos \alpha_n x_2 + B_{n,2} \sin \alpha_n x_2 & (0 \le x_2 \le l_2) \\ \quad \cdots & \quad \cdots \\ A_{n,i} \cos \alpha_n x_i + B_{n,i} \sin \alpha_n x_i & (0 \le x_i \le l_i) \\ \quad \cdots & \quad \cdots \\ A_{n,2p+1} \cos \alpha_n x_{2p+1} + B_{n,2p+1} \sin \alpha_n x_{2p+1} & (0 \le x_{2p+1} \le l_{2p+1}). \end{cases} \tag{16}$$

Of course, in Eq. (16), the range of global variable x is $0 \le x \le l_1$ in the first row, $l_1 \le x \le l_1 + l_2$ in the second one, $l_1 + l_2 + \cdots + l_{i-1} \le x \le l_1 + l_2 + \cdots + l_{i-1} + l_i$ in the i-th row and so on; for the last row it results: $l_1 + l_2 + \cdots + l_{2p} \le x \le l_1 + l_2 + \cdots + l_{2p} + l_{2p+1}$. The arbitrariness of the amplitude factor used to define $\mathbf{X}_n$ is inherited also by the corresponding eigenmode $\Psi_n(x)$ constructed in this way. As an example, those shown in Figure 3, which are relevant to an actual six complete span catenary corresponding to 13 single spans in the model (where the first and the last one have their outer end fixed) have been normalized in such a way that the maximum displacement is unitary.

The general solution of Eq. (2) can be expressed as a series of eigenmodes $\Psi_n(x)$ multiplied by time dependent coefficients $g_n(t)$:

$$y(x,t) = \sum_{n=1}^{\infty} \Psi_n(x) g_n(t). \tag{17}$$

Please cite this document as: A. Cazzani, M. Cattani, R. Mauro, F. Stochino "A simplified model for railway catenary-wire dynamics " *European Journal of Environmental and Civil Engineering* , 2017, 21(7–8): 936–959
DOI:10.1080/19648189.2016.1245631

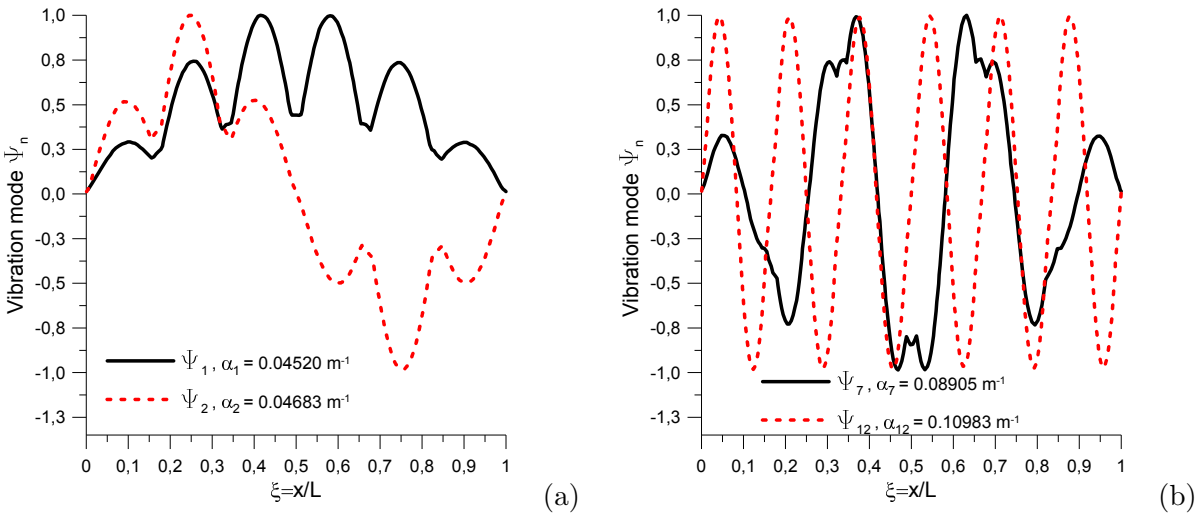

Figure 3. Eigenmodes number 1, 2 (a), 7 and 12 (b) for a six-span catenary.

Substituting Eq. (17) into Eq. (2) and taking into account Eqs. (6)–(7) yields:

$$\sum_{n=1}^{\infty} \left(m\Psi_n(x)\ddot{g}_n(t) + \omega_n^2 m\Psi_n(x)g_n(t) \right) = p(x,t). \tag{18}$$

The following well known orthogonality properties hold for the eigenfunctions of a taut string having a span length L:

$$\int_0^L \Psi_n(x)\Psi_k(x)dx = 0 \qquad \text{if} \quad n \neq k, \tag{19}$$

and

$$\int_0^L \Psi_n'(x)\Psi_k'(x)dx = 0 \qquad \text{if} \quad n \neq k. \tag{20}$$

So, multiplying the whole Eq. (18) by $\Psi_k(x)$ and integrating it along the string span, taking advantage of the above mentioned orthogonality properties (see Eq. (19)), provides an infinite number of decoupled equations of motion (one for each mode). Each of these equations can be solved independently, obtaining the unknown functions $g_n(t)$:

$$\ddot{g}_n(t) + \omega_n^2 g_n(t) = \frac{\int_0^L p(x,t)\Psi_n(x)dx}{\int_0^L m\Psi_n^2(x)dx}. \tag{21}$$

It is possible to take into account the effect of a single constant point load equal to $\hat{F}$ which is moving at a constant speed v along the wire if the vertical load distribution $p(x,t)$ is assumed to be a *generalized function* like this:

$$p(x,t) = \hat{F}\delta(x - vt), \tag{22}$$

where δ represents Dirac's delta distribution; with these assumptions and considering

Please cite this document as: A. Cazzani, M. Cattani, R. Mauro, F. Stochino "A simplified model for railway catenary-wire dynamics " *European Journal of Environmental and Civil Engineering* , 2017, 21(7–8): 936–959
DOI:10.1080/19648189.2016.1245631

the integral properties of δ, the right hand side of Eq. (21) becomes:

$$\frac{\int_0^L \hat{F}\delta(x-vt)\Psi_n(x)dx}{\int_0^L m\Psi_n^2(x)dx} = \hat{F}\frac{\Psi_n(vt)}{M_n}, \tag{23}$$

where $\Psi_n(vt)$ means the value of the eigenmode at position $x = vt$, and the following definition of generalized mass M_n has been introduced:

$$M_n = \int_0^L m\Psi_n^2(x)dx.$$

If Eq. (23) is substituted into Eq. (21) it yields an equation whose solution can be obtained by the following convolution integral, also known as Duhamel's integral (for details see, for instance, Bishop and Johnson (1960)):

$$g_n(t) = \frac{1}{\omega_n M_n}\hat{F}\int_0^t \Psi_n(v\tau)\sin\omega_n(t-\tau)d\tau. \tag{24}$$

In general, to properly take into account energy dissipation, viscous damping is introduced; in particular, this is often done directly in the modal equation of motion, Eq. (21), which is substituted by the following one:

$$\ddot{g}_n(t) + 2\nu_n\omega_n\dot{g}_n(t) + \omega_n^2 g_n(t) = \frac{\int_0^L p(x,t)\Psi_n(x)dx}{\int_0^L m\Psi_n^2(x)dx}, \tag{25}$$

where the so called modal damping factor ν_n appears. Thus for the case of a constant, vertical traveling force, moving at a constant speed v, when the contribution of modal viscous damping, characterized by a modal damping factor ν_n and by a modal damped angular frequency $\Omega_n = \omega_n\sqrt{1-\nu_n^2}$ is taken into account, the general solution of Eq. (2) becomes:

$$y(x,t) = \sum_{n=1}^{\infty}\hat{F}\frac{\Psi_n(x)}{M_n\Omega_n}\int_0^t \Psi_n(v\tau)\exp(-\nu_n\omega_n(t-\tau))\sin\Omega_n(t-\tau)d\tau. \tag{26}$$

4. Model description and calibration

The adopted model was developed to represent the dynamic behavior of a railway catenary system. The main simplification is the reduction to one wire only, when the real system consists of a straight contact wire and a curved one, the catenary, to which the former is hung at some discrete points, by means of droppers. The equivalent single wire should have the same displacement time-history of the actual contact wire, but it must also represent the whole system. The catenary rope is represented in the model as a distributed elastic support that plays an important role in the equivalent single wire dynamics. Indeed the effect of a vertical upward force on the equivalent wire displacements results in a smooth deformed curve. Without the continuous elastic support (a Winkler type one) this does not occur because the wire configuration would be a polygonal line. In the actual structure the droppers, which connect the contact wire to the catenary rope, would spread the effect of the point load along the whole catenary: this is approximated in the model by the continuous elastic support.

Please cite this document as: A. Cazzani, M. Cattani, R. Mauro, F. Stochino "A simplified model for railway catenary-wire dynamics " *European Journal of Environmental and Civil Engineering* , 2017, 21(7–8): 936–959
DOI:10.1080/19648189.2016.1245631

Generally speaking the static response to a static vertical force of the real catenary is nonlinear. This can be explained three ways: first, the self weight of the wire (which is indeed a heavy string) should not be disregarded since it perturbs the undeformed configuration of the catenary producing a nonlinear behavior; secondly even without taking into account the self weight, the response of a taut (straight) string depends nonlinearly on its prestress; finally the droppers produce a unilateral response in the real system. In the present case, however, a dead load similar to the upward force applied by the pantograph is supposed to produce very small displacements, such that the assumption that the response is almost insensitive to nonlinearities is still acceptable.

The concentrated elastic supports, due to the springs whose stiffness is K (see Figure 2), represent the stiffer behavior of the droppers near the support piles. Indeed droppers are directly connected to the catenary rope whose displacements close to the piles are restricted.

The mass per unit length of the wire in the model must also take into account the mass of the catenary rope. Combined, the overall value is larger than it would have been if only the real contact wire had been taken into account; thus the model inertia will be similar to the inertia of the actual complete catenary system.

Modeling the traction force also requires accounting for the effect of the catenary rope. Indeed, the wave speed in the contact wire depends only on the ratio between the traction force, T, and the linear density (mass per unit length) of the wire, m. For this reason this ratio T/m is crucial and must be evaluated carefully in order to capture accurately such dynamic phenomena.

The case study considered in this paper refers to a catenary model adopted by the Italian railways, a typical span of which is shown in Figure 4. It consists of a catenary rope, suspended between points O_1 and O_2, which is connected to an almost horizontal contact wire by a sequence of ten droppers.

4.1 *Finite Element reference model*

A FE model of the railway structure has been developed by means of the commercial software ABAQUS^{TM}. The three components of the system (catenary rope, droppers and contact wire) have been modeled by 2-noded truss elements labeled `T2D2` in the manual, see Dassault Systèmes (2015). This choice produces in each element a linear interpolation for position and displacements while stresses are constant. The dynamic analysis is performed taking into account finite strain, so that geometric nonlinearities are accounted for. The mesh consists of 600 elements for the catenary rope, 600 for the contact wire and one element for each of the 10 droppers which are present in any complete span. So for a six span model a grand total of 7260 elements have been considered. This value was obtained after a thorough investigation about the convergence properties of the modal analysis. A prestress force T has been applied to both the contact wire and the catenary rope; all wires are made of copper whose Young's modulus is $E = 117.7$ GPa. The other geometric and mechanical characteristics for each constituent are the following:

- Catenary rope: cross section area $A_1 = 155$ mm^2, mass per unit length $m_1 = 1.42$ kg/m, applied prestress traction $T_1 = 18.394$ kN.
- Contact wire: cross section area $A_2 = 150$ mm^2, mass per unit length $m_2 = 1.35$ kg/m, applied prestress traction $T_2 = 14.715$ kN.
- Dropper: cross section area $A_3 = 20$ mm^2, mass per unit length $m_3 = 0.18$ kg/m, $T_3 = 0.000$ kN, *i.e.* no applied prestress traction.

Please cite this document as: A. Cazzani, M. Cattani, R. Mauro, F. Stochino "A simplified model for railway catenary-wire dynamics " *European Journal of Environmental and Civil Engineering* , 2017, 21(7–8): 936–959
DOI:10.1080/19648189.2016.1245631

4.2 *Calibration of parameters*

For model calibration the following parameters have been considered: the total span length L, the distance between the catenary suspension point (denoted by O_1, O_2 in Figure 4) and the elastic support corresponding to the first dropper L_3 (expressed as a ratio, $\xi = L_3/L$, of the span length L), the traction force T, the wire mass per unit length m, the stiffness coefficients K (concentrated elastic support) and k (continuous elastic support), the modal damping ratio ν_n, which has been considered equal for all modes. Given the railway catenary geometry, which defines the values L and ξ, the remaining unknown parameters must be evaluated by comparing the simplified model with the above mentioned FE one. Comparison has been developed both in a static and in a dynamic range. In the first case the stiffness coefficients have been estimated in order to reduce the differences in terms of vertical displacements between the two models. More specifically, the two parameters K and k have been computed in order to minimize, by a least-squares approach, the quadratic norm of the difference between the FE and the simplified model displacements:

$$E(K,k) = \sum_{i=1}^{N} \left(y_i^{FE} - y_i^{sm}(K,k)\right)^2, \tag{27}$$

where y is the vertical displacement and N is a fixed number of points where such displacement difference has been evaluated. Figure 6 presents in a graphic way the resulting vertical stiffness value for the each point along the complete span for both the FE model and the simplified one.

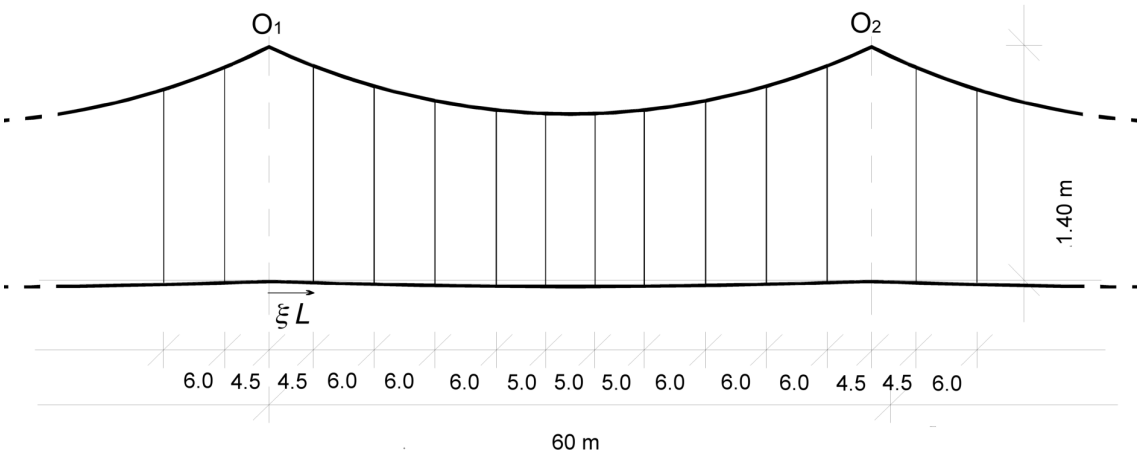

Figure 4. Sketch of a typical span of the Italian railway catenary; different scales are used for horizontal and vertical directions.

Dynamic comparison has been instead used for determining the equivalent linear mass density m. The selected value has been chosen again by a least-squares approach which involves minimizing the quadratic difference $E(m)$ between the numerical eigenfrequency ω_i^{FE} and the corresponding one $\omega_i^{sm}(m)$ obtained by the simplified model:

$$E(m) = \sum_{i}^{N} \left(\frac{\omega_i^{FE}(m) - \omega_i^{sm}}{\omega_i^{FE}} \right)^2. \tag{28}$$

Finally, the value of the prestress traction force T has been selected in order to keep

Please cite this document as: A. Cazzani, M. Cattani, R. Mauro, F. Stochino "A simplified model for railway catenary-wire dynamics " *European Journal of Environmental and Civil Engineering* , 2017, 21(7–8): 936–959
DOI:10.1080/19648189.2016.1245631

constant the ratio T/m of the contact wire (as it happens in the real system) so that the speed of wave propagation c in the wire itself does not change; it is useful to recall that c is linked to traction force T and to the mass density per unit length m by this equation: $c^2 = T/m$.

With the procedure outlined above it has been possible to completely characterize the geometric and the mechanical properties of the simplified model. They are: complete span length $L = 60$ m; span length fraction corresponding to the location of the first dropper $\xi = 0.075$; linear mass density (mass per unit length) $m = 2.11$ kg/m; prestress traction $T = 22999$ N; stiffness of the concentrated elastic support corresponding to the first dropper $K = 2429.2$ N/m; stiffness of the continuous elastic support $k = 30.026$ N/m^2; modal damping ratio $\nu = 0.02$, equal for all considered modes.

5. Model validation

The results obtained with the simplified model have been compared to those produced by the finite element code when a vertical upward constant force moving in the horizontal direction at a constant speed v on the equivalent straight single wire (representing the effect of the pantograph) has been considered. The geometry of the system is defined in Figure 5.

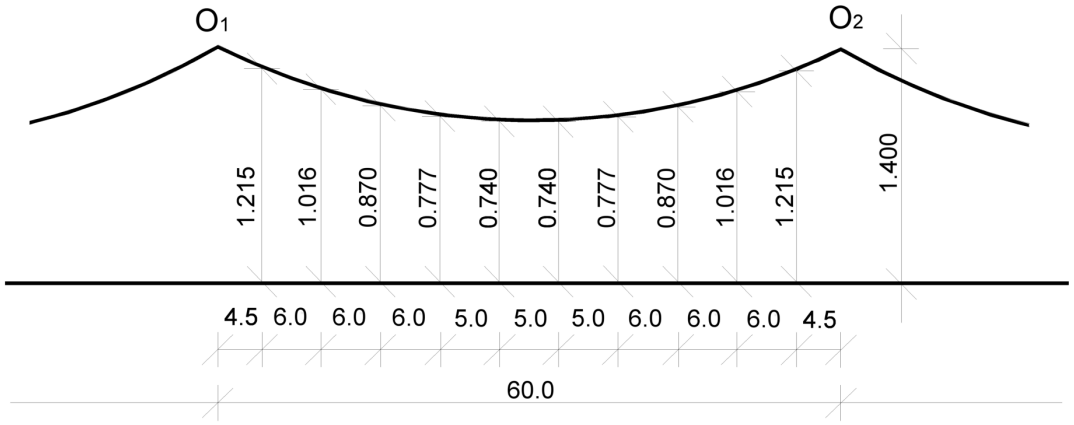

Figure 5. Simplified sketch of a typical span of the railway catenary which was considered for the analysis. Different scales are used for horizontal and vertical directions.

For the FE model, the propagation of a singular traveling constant force applied on the contact wire has been simulated by a suitable combination of nodal forces.

The vertical displacement has been evaluated at some selected points by means of the FE model and by the simplified one. In Figure 7 and Figure 8 the time-history of the vertical displacement of a midspan point and of a point close to the concentrated elastic support are reported respectively. The traveling speed of the load is $v = 70$ m/s (*i.e.* 252 km/h corresponding to a high-speed train). These diagrams highlight a good agreement between the FE numerical results and those obtained by the simplified model. In particular very small errors are found for the first eigenmodes at low frequencies. As frequencies become higher, an increase of these differences is experienced. This can be explained by the absence of the droppers which, instead, strongly influence higher eigenmodes in the complete model. Indeed droppers are located at a comparatively small distance and have the effect of producing a dynamic coupling between the catenary and

Please cite this document as: A. Cazzani, M. Cattani, R. Mauro, F. Stochino "A simplified model for railway catenary-wire dynamics " *European Journal of Environmental and Civil Engineering* , 2017, 21(7–8): 936–959
DOI:10.1080/19648189.2016.1245631

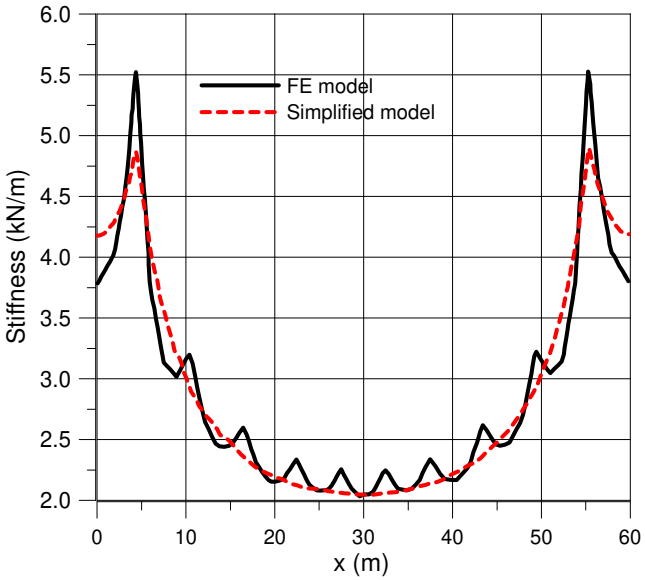

Figure 6. Comparison between FE and simplified model stiffness as a function of position along a complete catenary span.

the contact wire, which becomes of paramount relevance with high-frequency and short waves lengths.

For the sake of synthesis the simplified model produced quite good results, with an average error below 10% in comparison to the FE model but at a highly reduced computational cost.

6. Parametric analysis on the catenary dynamics

The reduced computational cost of the simplified model allows studying the influence of several parameters on the dynamic response of the system. Parameters whose importance is expected to be relevant are, for instance, the value of the traveling force, its traveling speed, the presence of more than one force and the corresponding distance. Such analyses might be useful in order to determine which are the most critical conditions for the system particularly in case of high speed trains. A central issue is the distance between the two pantographs, which are usually employed at the same time in the high speed train. Indeed the second pantograph may magnify or reduce wire vibrations caused by the first one depending on the catenary characteristics, but also on the distance between the two pantographs and the traveling speed.

The influence of some of the outlined parameters has been analyzed and are described in the following subsections.

Please cite this document as: A. Cazzani, M. Cattani, R. Mauro, F. Stochino "A simplified model for railway catenary-wire dynamics " *European Journal of Environmental and Civil Engineering* , 2017, 21(7–8): 936–959
DOI:10.1080/19648189.2016.1245631

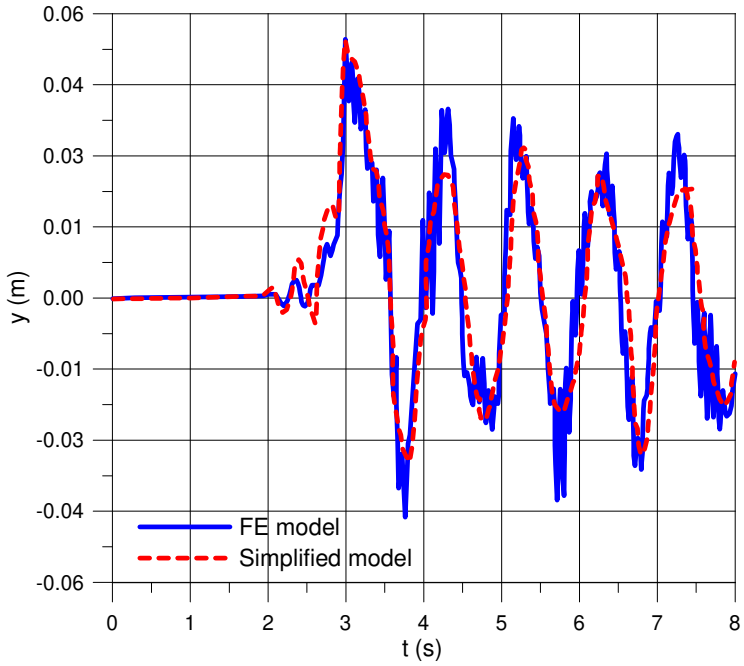

Figure 7. Comparison, in terms of time history, of the vertical displacement at a midspan point (span n. 4: $x = 210$ m) obtained by the FE model and by the simplified one. The traveling speed of the constant force is $v = 70$ m/s.

6.1 *Influence of the traveling speed on the catenary response*

The effect of constant traveling speed due to a single moving force (corresponding to a single pantograph) on vertical displacements of the power supplying system has been analyzed. In particular, the speed range between $v = 40$ m/s and $v = 120$ m/s has been explored. The upper bound has been selected considering the higher frequencies of the catenary. Indeed the vibration waves propagate along the wire, in both direction, at a fixed speed equal to $c = \sqrt{T/m} = 104.4$ m/s (or $c = 375.9$ km/h), for the considered mechanical model. In the following this value will be labelled as the *wave speed*. Thus it is interesting to investigate what happens when the force traveling speed is close to this value, in order to explore possible resonance effects. The maximum displacements values for 121 points, located 1.5 m apart along the spans number 3, 4 and 5, have been recorded during the time interval necessary to have one complete oscillation. For each point the maximum displacement y_{max} has been related to the corresponding traveling speed v. In this way two curves, labeled y^+_{max} and y^-_{max} have been obtained, see Figure 9. The former represents the *upper bound* of the maximum displacements (which is never exceeded

Please cite this document as: A. Cazzani, M. Cattani, R. Mauro, F. Stochino "A simplified model for railway catenary-wire dynamics " *European Journal of Environmental and Civil Engineering* , 2017, 21(7–8): 936–959
DOI:10.1080/19648189.2016.1245631

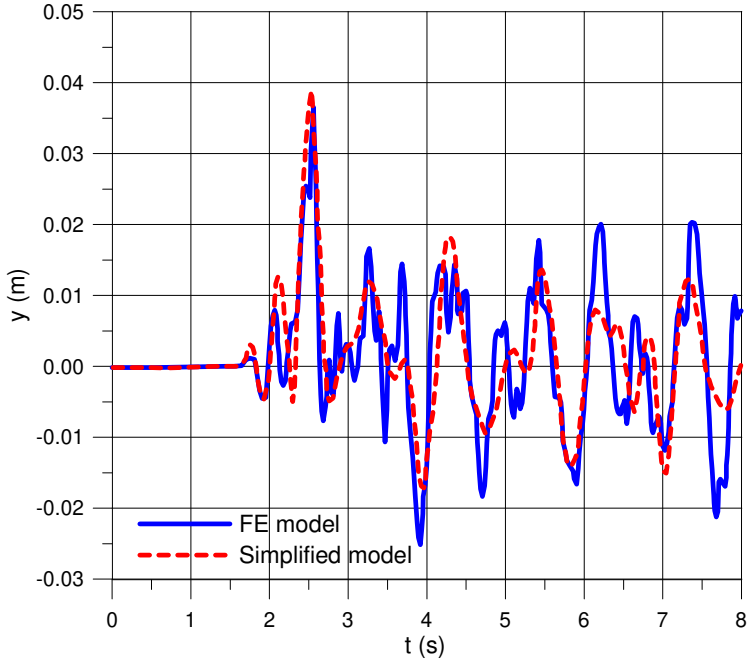

Figure 8. Comparison, in terms of time history, of the vertical displacement for a point close to a concentrated elastic support (span n. 3–4; $x = 180$ m) obtained by the FE model and by the simplified one. The traveling speed of the constant force is $v = 70$ m/s.

in any point of the system), while the latter represents the value of the transversal displacement that every point is expected to experience at least once during the analysis. These two curves measure the amplitude of the vibration range as a function of the force traveling speed, v.

The effect of this parameter is quite limited up to $v = 90$ m/s (*i.e.* $v = 324$ km/h). In particular, in same cases (look for example at what happens when the transition speed increases from $v = 60$ m/s to $v = 70$ m/s), an improvement of the transition speed corresponds to a reduction of the vertical displacement. It seems that for the analyzed case no critical events occur for the system even with transition speed around $v = 200$ km/h (namely, $v = 55$ m/s). Instead, when it goes closer to the wave speed of propagation, c, the wire vertical displacements increase vividly. For example, the maximum vertical displacement for a traveling speed $v = 105$ m/s is more than twice the maximum displacement for $v = 90$ m/s. This critical situation becomes less (but still) dangerous as the traveling speed becomes higher than the wave speed: in this case the perturbation produced by the transit of pantograph is quicker than the wave speed c as it occurs in

Please cite this document as: A. Cazzani, M. Cattani, R. Mauro, F. Stochino "A simplified model for railway catenary-wire dynamics " *European Journal of Environmental and Civil Engineering* , 2017, 21(7–8): 936–959
DOI:10.1080/19648189.2016.1245631

an ipersonic regime.

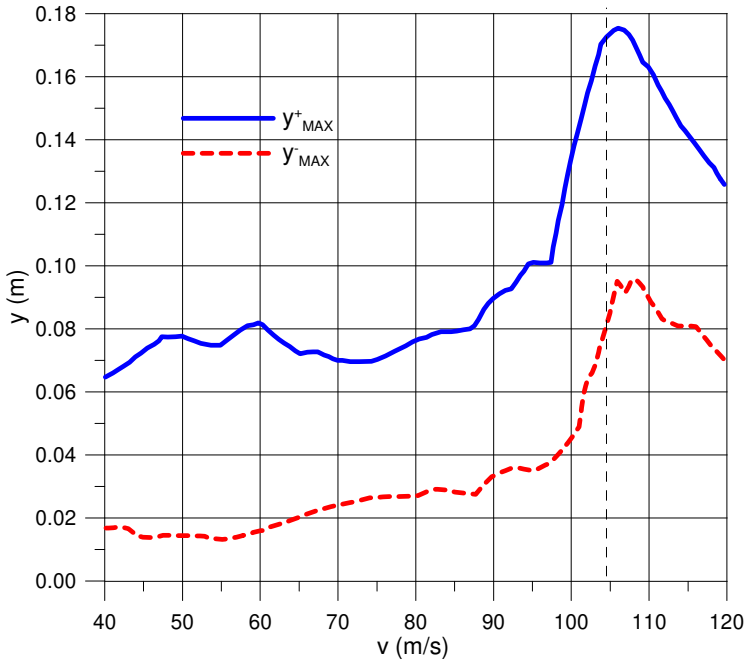

Figure 9. Bounds of the maximum displacements of the equivalent wire with a single pantograph ($\hat{F} = 200$ N), the dotted vertical line corresponds to the wave speed.

With the results presented in Figure 9 it can be proven that the traveling speed of the train v must be kept well under the wave speed c along the contact wire. When v is higher than 300–350 km/h (corresponding to 83–97 m/s) the use of catenary with different characteristics is required, for instance a wire with smaller density m or larger prestress force T in order to push up the wave speed c.

A similar analysis has been developed in the case of two consecutive pantographs separated by a distance $d = 241$ m (this is the case of an Italian high-speed train, specifically model ETR 500). The bounds of maximum displacements for this case are reported in Figure 10. Differently from what happened before, there are some lower values of the traveling speed (around 55 m/s) which corresponds to displacements peaks. For this velocity the perturbation produced by the first pantograph has the same frequency as that due to the second one, thus producing an internal resonance. When higher velocities are envisaged, the behavior becomes similar to that due to a single pantograph.

Please cite this document as: A. Cazzani, M. Cattani, R. Mauro, F. Stochino “A simplified model for railway catenary-wire dynamics ” *European Journal of Environmental and Civil Engineering* , 2017, 21(7–8): 936–959
DOI:10.1080/19648189.2016.1245631

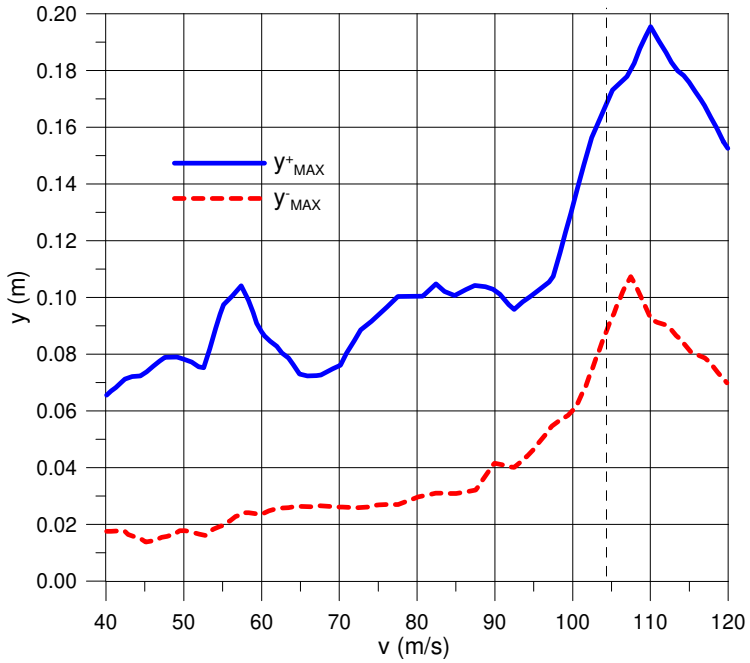

Figure 10. Bounds of the maximum displacements of the equivalent wire with two pantographs ($\hat{F}_1 = \hat{F}_2 = 200$ N; $d = 241$ m), the dotted vertical line corresponds to the wave speed.

6.2 *Influence of pantographs distance on the catenary response*

As pointed out before, when the train has two pantographs working together for supplying power to the engines they can interfere with each other. However the effect of the forward perturbation is limited. For example, looking at Figures 7 and 8 it is clear that significant displacements are recorded only after the pantograph transit. Before such transit, displacements are practically negligible. For this reason the first pantograph does not experience the presence of the second one, since it encounters a not-perturbed wire. On the other hand, the second pantograph finds a perturbed wire because the damping needs a longer time to become effective than that usually measured between the transit at a given position of both pantographs (approximately 4–5 s). Thus, the distance between the two pantographs (d) becomes an important parameter. Indeed d, along with the traveling speed v, determines how much, in a given position, the wire is perturbed when the second pantograph reaches it. If the second pantograph reaches that position when the vertical displacement exhibits an upward peak, the perturbation due to the second pantograph will produce a magnification of such displacement, resulting in a deteriorated

Please cite this document as: A. Cazzani, M. Cattani, R. Mauro, F. Stochino "A simplified model for railway catenary-wire dynamics " *European Journal of Environmental and Civil Engineering* , 2017, 21(7–8): 936–959
DOI:10.1080/19648189.2016.1245631

performance of the power supply system. Instead, if the second pantograph reaches the position when the vertical displacement has a downward peak, it will contribute to reduce the amplitude of vibration producing a globally better performance.

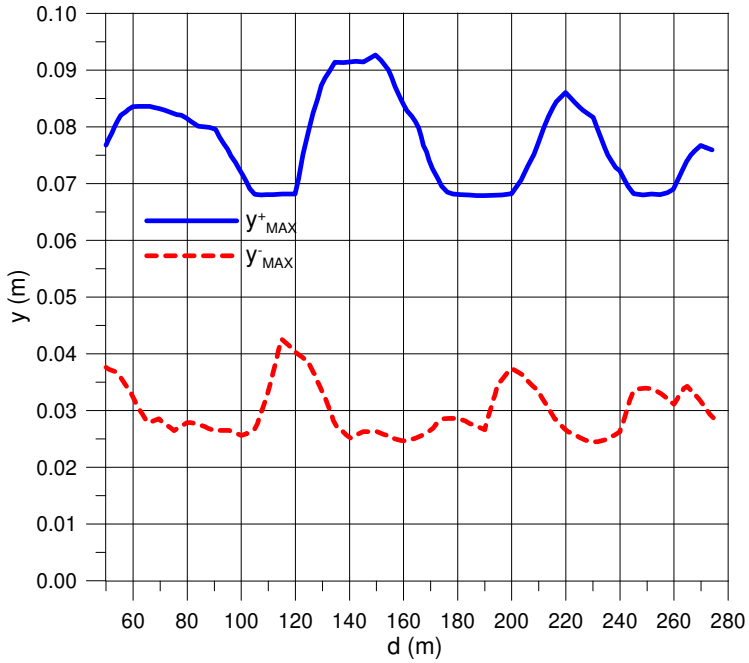

Figure 11. Bounds of the maximum displacements of the equivalent wire as a function of the distance between the two pantographs ($\hat{F}_1 = \hat{F}_2 = 200$ N; $v = 70$ m/s).

In order to find which is the best distance to have conveniently reduced displacements a parametric study has been developed by means of the simplified model. A fixed traveling speed $v = 70$ m/s has been considered while the distance between the two pantographs has been changed from $d = 50$ m to $d = 275$ m. This allowed to explore the working condition of the ETR trains whose pantograph distance can be either $d = 241$ m or $d = 267$ m, see Bianchi, Tacci, and Vandi (1991). As it has been done before, in Figure 11 the maximum displacements of all points of the equivalent wire located between spans number 3 and 4 (150 m $\leq x \leq 210$ m) are plotted as a function of the distance between pantographs. It can be noticed that there are some distances which correspond to a minimum value of displacements. In particular there are some distance ranges (see for example, from $d = 105$ m to $d = 110$ m) where the maximum displacement is constant. This can be explained by considering that the perturbation of the second pantograph

Please cite this document as: A. Cazzani, M. Cattani, R. Mauro, F. Stochino "A simplified model for railway catenary-wire dynamics " *European Journal of Environmental and Civil Engineering* , 2017, 21(7–8): 936–959
DOI:10.1080/19648189.2016.1245631

becomes negligible. Indeed the same values are obtained considering only one pantograph. These particular distance ranges appear to be optimal for the train operating conditions when the traveling speed is $v = 70$ m/s.

It is important to highlight that the interaction between the two pantograph depends on the time interval between their transits. Thus, only knowing the train speed it is possible to find the optimum distance which, of course, depends on that speed. For example, the optimal distance at a speed $v = 70$ m/s would be not favorable if the traveling speed reduces to $v = 60$ m/s.

7. Conclusion

The dynamic problem of a railway catenary has been solved with a simplified model in order to analyze the influence of some of the most meaningful parameters. The model is based on some assumptions which yield to a closed-form solution based on a series expansion of eigenfunctions.

The model has been validated by comparison with more refined numerical model, with reference to the time-history of the vertical displacements. The computational cost of the simplified model is conveniently low and this allows to develop useful parametric analyses, like those presented here.

Further developments of this research work and of the applications presented herein might include the development of highly efficient finite element models for strings and cables based on the isogeometric analysis, which has been already adopted *e.g.* by Cuomo, Contrafatto, and Greco (2014) for solids, and by Cazzani, Malagù, and Turco (2014), Cazzani, Malagù, and Turco (2014), Cazzani et al. (2016a), Chiozzi et al. (2016), Cazzani, Stochino, and Turco (2016a), Greco and Cuomo (2016) for straight and curved beams. In particular, beam vibration problems treated by the isogeometric approach have been addressed recently by Greco and Cuomo (2015), Cazzani, Stochino, and Turco (2016b), Cazzani, Stochino, and Turco (2016c). On the other hand, the present research could be extended by applying to the catenary-wire those peculiar methods for the study of buckling and dynamic stability which have been developed, for instance, for the case of thin walled structures by Ruta et al. (2008), Pignataro et al. (2009), Pignataro et al. (2010), Rizzi and Varano (2011a), Rizzi and Varano (2011b), Rizzi, Varano, and Gabriele (2013). In addition, in order to capture possible necking and kinking effects arising from catenary-pantograph interaction, the approach presented in AminPour and Rizzi (2016) could be usefully employed.

Finally, further research perspectives could be conceived taking into account the damage of supports which involves a change of the dynamic parameters of the entire structure examined and then a different behavior of the same (see, e.g., Contrafatto, Cuomo, and Fazio (2012), Cuomo and Nicolosi (2006), Contrafatto, Cuomo, and Di Venti (2012)) for models which address such an issue.

Appendix A.

Looking at the complete Eq. (4) (including the case $k \neq 0$) it is possible to separate functions depending on time t from those depending on space x obtaining:

$$\frac{T\,\Psi''(x) - k\,\Psi(x)}{m\,\Psi(x)} = \frac{\ddot{g}(t)}{g(t)}. \tag{A1}$$

Please cite this document as: A. Cazzani, M. Cattani, R. Mauro, F. Stochino "A simplified model for railway catenary-wire dynamics " *European Journal of Environmental and Civil Engineering* , 2017, 21(7–8): 936–959
DOI:10.1080/19648189.2016.1245631

The l.h.s. and the r.h.s. of Eq. (A1), depend on different variables. In order to be equal, they must yield a common constant, which will be labeled $-\omega^2$. Consequently:

$$\frac{T\,\Psi'' - k\,\Psi}{m\,\Psi} = \frac{\ddot{g}}{g} = -\omega^2. \tag{A2}$$

It is possible to show that the constant value $-\omega^2$ occurring in Eq. (A2) must indeed be negative. This can be checked if both sides of the equation which provides Ψ, namely:

$$T\,\Psi'' - k\,\Psi = -\omega^2 m\,\Psi$$

are multiplied by Ψ and then integrated between 0 and L:

$$\int_0^L T\,\Psi''\Psi dx - \int_0^L k\,\Psi^2 dx = -\omega^2 \int_0^L m\,\Psi^2 dx. \tag{A3}$$

In order to show that Eq. (A3) holds, the left hand side must be negative. By the way, it should be noticed that the term $\int_0^L m\,\Psi^2 dx > 0$ appearing in the r.h.s. is related to the kinetic energy of the system, while the last term in the l.h.s. $\int_0^L k\,\Psi^2 dx > 0$ is similarly connected to the strain energy associated to the continuous elastic support. Now if integration by parts is applied to the first term in the l.h.s. of Eq. (A3), it can be transformed as follows:

$$\int_0^L T\,\Psi''\Psi dx = \left(T\,\Psi'\Psi\right)\Big|_0^L - \int_0^L T\,\left(\Psi'\right)^2 dx, \tag{A4}$$

where the last term in the r.h.s., $\int_0^L T\,\left(\Psi'\right)^2 dx > 0$ is linked to the strain energy of the wire. Next, it has to be noticed that the most common boundary conditions, ensure that $T\,\Psi'\Psi(x)\big|_0^L$ vanishes: indeed, for a fixed end $\Psi = 0$, while for a free end $T\,\Psi' = 0$; as a consequence any possible combination of fixed and/or free ends yields:

$$\left(T\,\Psi'\Psi\right)\Big|_0^L = 0. \tag{A5}$$

In the most general case of elastically supported ends (hence when springs with $K \neq 0$ are placed at both ends of the wire) the BCs become:

$$T\,\Psi'\big|_L = -K\,\Psi|_L; \qquad T\,\Psi'\big|_0 = +K\,\Psi|_0,$$

As a consequence:

$$\left(T\,\Psi'\Psi\right)\Big|_0^L = \left(-K\,\Psi^2|_L - K\Psi^2|_0\right) < 0. \tag{A6}$$

Therefore, it follows from Eqs. (A5)–(A6) that it results, in any case:

$$\int_0^L T\,\Psi''\Psi(x) dx < 0,$$

Please cite this document as: A. Cazzani, M. Cattani, R. Mauro, F. Stochino "A simplified model for railway catenary-wire dynamics " *European Journal of Environmental and Civil Engineering* , 2017, 21(7–8): 936–959
DOI:10.1080/19648189.2016.1245631

and Eq. (A1) holds always with $-\omega^2 < 0$. Thus, it is clear that the same leads to the following system of ODEs:

$$\begin{cases} T\,\Psi''(x) + (\omega^2 m - k)\Psi(x) = 0 \\ \ddot{g}(t) + \omega^2 g(t) = 0. \end{cases} \tag{A7}$$

Acknowledgement

The financial support of MIUR, the Italian Ministry of University and Research , under grant number PRIN-2010MBJK5B. (Progetti di Ricerca di Interesse Nazionale bando 2010–2011, Project *Dynamic, Stability and Control of Flexible Structures*) is gratefully acknowledged.

References

Acito, M., F. Stochino, and S. Tattoni. 2011. "Structural response and reliability analysis of RC beam subjected to explosive loading." *Applied Mechanics and Materials* 82: 434–439.

AminPour, H., and N. Rizzi. 2016. "A one-dimensional continuum with microstructure for single-wall carbon nanotubes bifurcation analysis." *Mathematics and Mechanics of Solids* 21 (2): 168–181.

Andreaus, U., P. Baragatti, and L. Placidi. 2016. "Experimental and numerical investigations of the responses of a cantilever beam possibly contacting a deformable and dissipative obstacle under harmonic excitation." *International Journal of Non-Linear Mechanics* 80: 96–106.

Andreaus, U., B. Chiaia, and L. Placidi. 2013. "Soft-impact dynamics of deformable bodies." *Continuum Mechanics and Thermodynamics* 25 (2–4): 375–398.

Andreu, A., L. Gil, and P. Roca. 2006. "A new deformable catenary element for the analysis of cable net structures." *Computers & Structures* 84: 1882–1890.

Andrews, H.I. 1964. "Third Paper: calculating the behaviour of an overhead catenary system for railway electrification." *Proceedings of the Institution of Mechanical Engineers* 179 (1): 809–846.

Arnold, M., and B. Simeon. 2000. "Pantograph and catenary dynamics: a benchmark problem and its numerical solution." *Applied Numerical Mathematics* 34 (4): 345–362.

Becker, K., A. König, U. Resch, and B.-W. Zweig. 1995. "Hochgeschwindigkeitsfahrleitung: Ein Thema für die Forschung." *ETR — Eisenbahntechnische Rundschau* 44 (1–2): 64–72.

Berezovski, A., I. Giorgio, and A. Della Corte. 2016. "Interfaces in micromorphic materials: Wave transmission and reflection with numerical simulations." *Mathematics and Mechanics of Solids* 21 (1): 37–51.

Bianchi, C., and G. Tacci. 1991. "Stromabnehmer für Gleichstrornbahnen." *Elektrische Bahnen* 89 (11): 429–435.

Bianchi, C., G. Tacci, and A. Vandi. 1991. "Studio dell'interazione dinamica di pantografi-catenaria con programma di simulazione agli elementi finiti. Verifiche sperimentali." *Ingegneria Ferroviaria* 46 (11): 647–667.

Bishop, R.E.D., and D.C. Johnson. 1960. *The Mechanics of Vibration*. Cambridge: Cambridge University Press.

Brodkorb, A., and M. Semrau. 1993. "Simulationsmodell des Systems Oberleitungskettenwerk und Stromabnehmer." *Elektrische Bahnen* 91 (4): 105–113.

Cattani, M., A.M. Cazzani, and R. Mauro. 2000. "Un modello semplificato della dinamica del filo di contatto." *Ingegneria Ferroviaria* 55 (11): 708–716.

Cazzani, A. 2013. "On the dynamics of a beam partially supported by an elastic foundation: An exact solution-set." *International Journal of Structural Stability and Dynamics* 13 (8): 1350045.

Cazzani, A., M. Malagù, and E. Turco. 2014. "Isogeometric analysis: a powerful numerical tool for

Please cite this document as: A. Cazzani, M. Cattani, R. Mauro, F. Stochino "A simplified model for railway catenary-wire dynamics " *European Journal of Environmental and Civil Engineering* , 2017, 21(7–8): 936–959
DOI:10.1080/19648189.2016.1245631

the elastic analysis of historical masonry arches." *Continuum Mechanics and Thermodynamics* 28 (1–2): 139–156.

Cazzani, A., M. Malagù, and E. Turco. 2014. "Isogeometric analysis of plane-curved beams." *Mathematics and Mechanics of Solids* 21 (5): 562–577.

Cazzani, A., M. Malagù, E. Turco, and F. Stochino. 2016a. "Constitutive models for strongly curved beams in the frame of isogeometric analysis." *Mathematics and Mechanics of Solids* 21 (2): 182–209.

Cazzani, A., F. Stochino, and E. Turco. 2016a. "An analytical assessment of finite element and isogeometric analyses of the whole spectrum of Timoshenko beams." *ZAMM - Journal of Applied Mathematics and Mechanics / Zeitschrift für Angewandte Mathematik und Mechanik* 1–25. DOI:10.1002/zamm.201500280.

Cazzani, A., F. Stochino, and E. Turco. 2016b. "On the whole spectrum of Timoshenko beams. Part I: a theoretical revisitation." *Zeitschrift für Angewandte Mathematik und Physik (ZAMP)* 67 (2): 24.

Cazzani, A., F. Stochino, and E. Turco. 2016c. "On the whole spectrum of Timoshenko beams. Part II: further applications." *Zeitschrift für Angewandte Mathematik und Physik (ZAMP)* 67 (2): 25.

Cazzani, A., N. Wagner, P. Ruge, and F. Stochino. 2016b. "Continuous transition between traveling mass and traveling oscillator using mixed variables." *International Journal of Non-Linear Mechanics* 80: 82–95.

Chiozzi, A., M. Malagù, A. Tralli, and A. Cazzani. 2016. "ArchNURBS: NURBS-based tool for the structural safety assessment of masonry arches in MATLAB." *ASCE Journal of Computing in Civil Engineering* 30 (2): 04015010.

Contrafatto, L., M. Cuomo, and G.T. Di Venti. 2012. "Finite elements with non homogeneous embedded discontinuities." In *6th European congress on computational methods in applied sciences and engineering, ECCOMAS,* 35–46.

Contrafatto, L., M. Cuomo, and F. Fazio. 2012. "An enriched finite element for crack opening and rebar slip in reinforced concrete members." *International Journal of Fracture* 178 (1–2): 33–50.

Cuomo, M., L. Contrafatto, and L. Greco. 2014. "A variational model based on isogeometric interpolation for the analysis of cracked bodies." *International Journal of Engineering Science* 80: 173–188.

Cuomo, M., and A. Nicolosi. 2006. "A poroplastic model for hygro-chemo-mechanical damage of concrete." In *EURO-C; Computational modelling of concrete structures Conference,* 533–542.

Dassault Systèmes. 2015. *ABAQUS 6.14 Documentation — Theory Guide*. Providence, RI: Dassault Systèmes.

dell'Isola, F., A. Della Corte, I. Giorgio, and D. Scerrato. 2016a. "Pantographic 2D sheets: Discussion of some numerical investigations and potential applications." *International Journal of Non-Linear Mechanics* 80: 200–208.

dell'Isola, F., I. Giorgio, and U. Andreaus. 2015. "Elastic pantographic 2D lattices: A numerical analysis on the static response and wave propagation." *Proceedings of the Estonian Academy of Sciences* 64 (3): 219–225.

dell'Isola, F., I. Giorgio, M. Pawlikowski, and N.L. Rizzi. 2016b. "Large deformations of planar extensible beams and pantographic lattices: heuristic homogenization, experimental and numerical examples of equilibrium." *Proc. R. Soc. A* 472 (2185): 20150790.

dell'Isola, F., A. Madeo, and L. Placidi. 2012. "Linear plane wave propagation and normal transmission and reflection at discontinuity surfaces in second gradient 3D continua." *ZAMM - Journal of Applied Mathematics and Mechanics / Zeitschrift für Angewandte Mathematik und Mechanik* 92 (1): 52–71.

Ding, Z. 1993. "A general solution to vibrations of beams on variable Winkler elastic foundation." *Computers & Structures* 47 (1): 83–90.

Eremeyev, V.A., E.A. Ivanova, N.F. Morozov, and S.E. Strochkov. 2007. "The spectrum of natural oscillations of an array of micro- or nanospheres on an elastic substrate." *Doklady Physics* 52 (12): 699–702.

Ferretti, M., and G. Piccardo. 2013. "Dynamic modeling of taut strings carrying a traveling mass." *Continuum Mechanics and Thermodynamics* 25 (2–4): 469–488.

Please cite this document as: A. Cazzani, M. Cattani, R. Mauro, F. Stochino "A simplified model for railway catenary-wire dynamics " *European Journal of Environmental and Civil Engineering* , 2017, 21(7–8): 936–959 DOI:10.1080/19648189.2016.1245631

Gilbert, G., and H.E.H. Davies. 1966. "Pantograph motion on a nearly uniform railway overhead line." *Proceedings of the Institution of Electrical Engineers* 113 (3): 485–492.

Greco, L., and M. Cuomo. 2015. "Consistent tangent operator for an exact Kirchhoff rod model." *Continuum Mechanics and Thermodynamics* 27 (4–5): 861–877.

Greco, L., and M. Cuomo. 2016. "An isogeometric implicit G1 mixed finite element for Kirchhoff space rods." *Computer Methods in Applied Mechanics and Engineering* 298: 325–349.

Greco, L., N. Impollonia, and M. Cuomo. 2014. "A procedure for the static analysis of cable structures following elastic catenary theory." *International Journal of Solids and Structures* 51 (7): 1521–1533.

Hamzaoui, F., F. Taillandier, R. Mehdizadeh, D. Breysse, and A. Allal. 2015. "Evolutive risk breakdown structure for managing construction project risks: application to a railway project in Algeria." *European Journal of Environmental and Civil Engineering* 19 (2): 238–262.

Hobbs, A.E.W., R. Illingworth, and A.J. Peters. 1977. "New developments in understanding the dynamics of overhead current collection equipment for electric railways." *Closed Loop* 1: 3–9.

Levy, S., J.A. Bain, and E.J. Leclerc. 1968. "Railway overhead contact systems, catenary-pantograph dynamics for power collection at high speeds." *ASME Journal of Manufacturing Science and Engineering* 90 (4): 692–699.

Lopez-Garcia, O., A. Carnicero, and V. Torres. 2006. "Computation of the initial equilibrium of railway overheads based on the catenary equation." *Engineering Structures* 28 (10): 1387–1394.

Madeo, A., A. Della Corte, L. Greco, and P. Neff. 2015. "Wave propagation in pantographic 2D lattices with internal discontinuities." *Proceedings of the Estonian Academy of Sciences* 64 (3S): 325–330.

Manabe, K., and Y. Fujii. 1990. "Resonanzen des Oberleitungssystems bei Verwendung von mehreren Stromabnehmem sowie Gegenmdnahmen." *Elektrische Bahnen* 88 (11): 403–409.

Metrikine, A.V., A.R.M. Wolfert, and A.C.W.M. Vrouwenvelder. 1999. "Steady-state response of periodically supported structures to a moving load." *Heron* 44 (2): 91–107.

Nibler, H. 1950. "Dynamisches Verhalten von Fahrleitung und Stromabnehmer bei elektrischen Hauptbahnen." *Elektrische Bahnen* 21 (10): 234–241.

Oda, O., T. Morikawa, and S. Kusumi. 1986. "Reduction method of contact losses of overhead-catenary and pantograph system." *Railway Technical Research Institute, Quarterly Reports* 27 (4): 115–120.

Park, T.-J., C.-S. Han, and J.-H. Jang. 2003. "Dynamic sensitivity analysis for the pantograph of a high-speed rail vehicle." *Journal of Sound and Vibration* 266 (2): 235–260.

Piccardo, G., L.C. Pagnini, and F. Tubino. 2015. "Some research perspectives in galloping phenomena: critical conditions and post-critical behavior." *Continuum Mechanics and Thermodynamics* 27 (1–2): 261–285.

Piccardo, G., F. Tubino, and A. Luongo. 2016. "Equivalent nonlinear beam model for the 3-D analysis of shear-type buildings: Application to aeroelastic instability." *International Journal of Non-Linear Mechanics* 80: 52–65.

Pignataro, M., N. Rizzi, G. Ruta, and V. Varano. 2009. "The effects of warping constraints on the buckling of thin-walled structures." *Journal of Mechanics of Materials and Structures* 4 (10): 1711–1727.

Pignataro, M., G. Ruta, N. Rizzi, and V. Varano. 2010. "Effects of warping constraints and lateral restraint on the buckling of thin-walled frames." *ASME International Mechanical Engineering Congress and Exposition, Proceedings* 10 (10 PART B): 803–810.

Poetsch, G., J. Evans, R. Meisinger, W. Kortüm, W. Baldauf, A. Veitl, and J. Wallaschek. 1997. "Pantograph/catenary dynamics and control." *Vehicle System Dynamics* 28: 159–195.

Reinbold, M., and U. Deckart. 1996. "FAMOS: Ein Programm zur Simulation von Oberleitungen und Stromabnehmern." *ZEV DET Glasers Annalen Die Eisenbahntechnik* 120 (6): 239–243.

Renger, A. 1990. "Berechnung des dynamischen Verhaltens von Oberleitungskettenwerkund Stromabnehmer." *VDI Berichte* 820: 141–154.

Resch, U. 1991. "Simulation des dynamischen Verhaltens von Oberleitungen und Stromabnehmem bei hohen Geschwindigkeiten." *Elektrische Bahnen* 89 (11): 445–446.

Rizzi, N.L., and V. Varano. 2011a. "The effects of warping on the postbuckling behaviour of thin-walled structures." *Thin-Walled Structures* 49 (9): 1091–1097.

Rizzi, N.L., and V. Varano. 2011b. "On the postbuckling analysis of thin-walled frames." *Proceed-*

Please cite this document as: A. Cazzani, M. Cattani, R. Mauro, F. Stochino "A simplified model for railway catenary-wire dynamics " *European Journal of Environmental and Civil Engineering* , 2017, 21(7–8): 936–959
DOI:10.1080/19648189.2016.1245631

ings of the 13th International Conference on Civil, Structural and Environmental Engineering Computing 1–14.

Rizzi, N.L., V. Varano, and S. Gabriele. 2013. "Initial postbuckling behavior of thin-walled frames under mode interaction." *Thin-Walled Structures* 68: 124–134.

Rosi, G., I. Giorgio, and V.A. Eremeyev. 2013. "Propagation of linear compression waves through plane interfacial layers and mass adsorption in second gradient fluids." *ZAMM - Journal of Applied Mathematics and Mechanics / Zeitschrift für Angewandte Mathematik und Mechanik* 93 (12): 914–927.

Rosi, G., J. Pouget, and F. dell'Isola. 2010. "Control of sound radiation and transmission by a piezoelectric plate with an optimized resistive electrode." *European Journal of Mechanics - A/Solids* 29 (5): 859–870.

Ruta, G.C., V. Varano, M. Pignataro, and N.L. Rizzi. 2008. "A beam model for the flexural-torsional buckling of thin-walled members with some applications." *Thin-Walled Structures* 46 (7-9): 816–822.

Scerrato, D., I. A. Zhurba Eremeeva, T. Lekszycki, and N. L. Rizzi. 2016. "On the effect of shear stiffness on the plane deformation of linear second gradient pantographic sheets." *ZAMM - Journal of Applied Mathematics and Mechanics / Zeitschrift für Angewandte Mathematik und Mechanik* DOI:10.1002/zamm.201600066.

Scott, P. R., and M. Rothman. 1974. "Computer evaluation of overhead equipment for electric railroad traction." *IEEE Transactions on Industry Applications* IA-10 (5): 573–580.

Seo, J.-H., S.-W. Kim, I.-H. Jung, T.-W. Park, J.-Y. Mok, Y.-G. Kim, and J.-B. Chai. 2006. "Dynamic analysis of a pantograph-catenary system using absolute nodal coordinates." *Vehicle System Dynamics* 44 (8): 615–630.

Stochino, F. 2016. "RC beams under blast load: Reliability and sensitivity analysis." *Engineering Failure Analysis* 66: 544–565.

Such, M., J.R. Jimenez-Octavio, A. Carnicero, and O. Lopez-Garcia. 2009. "An approach based on the catenary equation to deal with static analysis of three dimensional cable structures." *Engineering Structures* 31 (9): 2162–2170.

Veylon, G., and J. Gual. 2003. "Vibrations d'un hauban soumis á un vent turbulent." *Revue Française de Génie Civil* 7 (2): 195–220.

Wang, C.Y., and C.M. Wang. 2013. *Structural Vibration: exact solutions for strings, membranes, beams, and plates*. Boca Raton: CRC Press.

Wang, H.I., and S.-F. Qin. 2016. "Shape finding of suspension bridges with interacting matrix." *European Journal of Environmental and Civil Engineering* 20 (8): 831–840.

Wu, T.X., and M.J. Brennan. 1998. "Basic analytical study of pantograph-catenary system dynamics." *Vehicle System Dynamics* 30 (6): 443–456.

Wu, T.X., and M.J. Brennan. 1999. "Dynamic stiffness of a railway overhead wire system and its effect on pantograph-catenary system dynamics." *Journal of Sound and Vibration* 219 (3): 483–502.

Zulli, D., and A. Luongo. 2012. "Bifurcation and stability of a two-tower system under wind-induced parametric, external and self-excitation." *Journal of Sound and Vibration* 331 (2): 365–383.

Please cite this document as: A. Cazzani, M. Cattani, R. Mauro, F. Stochino "A simplified model for railway catenary-wire dynamics " *European Journal of Environmental and Civil Engineering* , 2017, 21(7–8): 936–959 DOI:10.1080/19648189.2016.1245631